Institute of Paper Science and Technology
Atlanta, Georgia

IPST Technical Paper Series Number 628

Acoustic Enhancement of Dry HCl Scrubbing with Calcium Oxide

J.R. Boerner and D.I. Orloff

October 1996

Submitted to
AIChE Annual Meeting
Chicago, Illinois
November 12, 1996

Acoustic Enhancement of Dry HCl Scrubbing with Calcium Oxide

J.R. Boerner
D.I. Orloff
Institute of Paper Science and Technology
500 10th St. NW
Atlanta, GA 30318
(404) 894 - 5700

ABSTRACT

Dry scrubbing of acidic gases is a common technique employed to clean flue gas resulting from combustion processes. It is capable of removing species such as SO_2 and HCl. A current disadvantage of dry scrubbing is incomplete conversion of the sorbent material, usually calcined limestone. Any improvement in reaction conversion between the sorbent and the acidic gas may lessen sorbent quantity requirements or decrease the size of the solid/gas contacting equipment, both of which are of high economic value.

Several examples in the literature show that processes conducted in an intense acoustic field can substantially improve chemical conversion between solid/gas reactions. Calcining and hazardous waste reduction are areas where acoustic field application has been shown to improve chemical conversion. This paper examines the effects of reactor temperature and CaO particle size on chemical conversion of HCl to $CaCl_2$ with and without an acoustic field.

Results of our entrained flow reactor studies show that reaction conversion increases with reactor temperature in the range 125 °C to 350 °C and with decreasing CaO particle size for three different size fractions possessing mass mean particle sizes of 90, 56 and 4μm. For the midsize CaO particles, chloride ion capture was improved up to 86% in an acoustic field of 163 dB (decibel) resonating between 600-750 Hz at 200 °C reactor temperature. No improvement in reaction conversion was found for the largest CaO particle fraction and only marginal improvement was noted in the cases involving the smallest CaO particles. Conversion enhancement may be due to greater concentration gradient of HCl around the CaO particles caused by enhanced mixing of the reactants resulting from the acoustic field.

1. Introduction

Scrubbing technology is used to remove acidic gases from combustion process stack gases. Scrubbers are typically an entrained flow configuration, but various embodiments of the scrubbing process are possible with the two main classifications being wet and dry methods. Wet and dry scrubbing methods remove acidic gases such as

SO_2 and HCl with calcium based sorbent compounds[1,2,3,4]. Wet scrubbing is accomplished by contacting a countercurrent flow of flue gas with a slaked lime/ground limestone slurry in an open or packed tower. The acidic gas is transferred from the gas to the liquid. The salt formed in the scrubbing reaction must be precipitated in a separate reaction vessel. This system is common among utility boilers and has the advantage of proven design and high removal efficiencies of the acidic gas component[2]. Disadvantages include high water consumption, corrosion potential, scale and plugging problems and sludge disposal difficulties[2].

Dry scrubbing utilizes a slurry of lime which is atomized into a fine mist that dries almost immediately upon injection into the flue gas where the acidic component reacts with the calcium compound to form a dry product[2,3]. In another embodiment of dry scrubbing the sorbent is injected directly into different sections of the furnace in powder form where it can react with the acidic gas[4]. Dry scrubbing possesses the advantages of a simpler process design, low pressure drop in the scrubbing system and a dry reaction product which contains the salt of the acid that can be more easily disposed compared with a sludge[2]. Even with these advantages dry scrubbing does not provide as high a removal rate of the acidic gas, a reason wet scrubbing methods are used more than dry scrubbing methods. An enhancement of gas scrubbing efficiency may improve the feasibility of use of dry scrubbing technology in order to use the advantages that the dry configurations offer.

Intense acoustic fields over 160 dB have been shown to improve some industrial-related reactions. Drying, incineration of municipal waste, coal combustion and calcination are examples of operations which can benefit from acoustic fields in the reaction vessel[5,6]. Documented laboratory scale work, with the exception of incineration of municipal waste which has been conducted on a pilot plant scale, shows significant process improvements due to the acoustic field[5,6]. This work began with the idea that a 160 dB acoustic field might also improve the efficiency of dry scrubbing and thus make it more advantageous in the removal of acidic gases from combustion processes.

In this investigation we are interested in a specific example of a type of reaction associated with dry scrubbers. The CaO/HCl reaction is of interest due to the recent work on this reaction to characterize temperature and particle size effects of the reaction[7,8,9,10]. The reaction proceeds as follows:

$$2HCl(g) + CaO(s) \longrightarrow CaCl_2(s) + H_2O(g)$$

However, the CaO/HCl reaction has been examined only with fixed bed systems requiring sample sizes on the order of a few grams. This past experience has uncovered some general reaction behavior between CaO and acidic gases such as reaction conversion increases with temperature and a decrease in sorbent particle diameter[8,9]. We will examine

an entrained flow reaction so results will have applicability to a general embodiment of dry scrubbing.

2. Experimental Apparatus

2.1 Entrained flow reactor

An entrained flow reactor (EFR), Figure 1, was designed to investigate reaction conversion of two-phase reactions. The EFR consists of a 3.8 cm inch diameter quartz reactor, a fluidized bed particle feeder, ammonia reaction quench, a computer interfaced data acquisition system and reaction product collection screen. Nitrogen carrier gas was preheated with an electric gas circulation heater which was introduced at the top of the reactor. Reaction temperature was maintained by three zones of radiant heaters controlled independently. Sorbent was injected into the carrier gas at the top of the reactor where it traveled through a 61 cm injection tube to achieve reactor temperature before contact with the gaseous reagent. The gas/solid mixture was quenched rapidly by an injection of NH_3 gas at the bottom section of the reactor called the decoupler. The reaction product passed through the decoupler and was accumulated in the collection cylinder.

The reactor tube is L-shaped allowing for introduction of the reactants and collection of the reaction products while maintaining a standing sound wave with a sound pressure maximum at approximately the tube center and pressure nodes approximately every 12 inches. A portion of the reactor was fitted with a series of quartz optical viewports for entry of a laser beam for conducting gas and particle velocity measurements. Thermocouple and pressure transducer ports are located on the vertical tube section for collecting temperature and sound pressure data. The reactor tubes are categorized into three sections; the acoustic section, mixing section and reactor section.

This EFR differs from conventional entrained flow reactors, as it was fitted with compression drivers which were attached on the tube walls to generate an intense resonant sound wave within the reactor tube. Additionally, the decoupler at the bottom of the reactor section dampens the sound pressure oscillations from the carrier gas and provides the necessary retention time to quench any unreacted HCl. The entire reactor tube was encased in a steel shell to channel leaks to the exhaust hoods to prevent gas leaks from invading the surrounding environment. The reactor may operate in a batch or continuous manner. Continuous operation was the mode in which the present experiments were conducted.

A fluidized bed feeder was used to inject the desired quantity of CaO into the reactor. The sorbent feeder was operated in a continuous mode for the reaction conversion experiments in both steady flow and with acoustics. Fluidization gas, tangential mixing gas and jet gas were monitored with rotameters to achieve a consistent feed rate of CaO. It is important to maintain consistent particle density in the reactor to allow comparison of steady flow reaction results to those obtained in an acoustic field. Particle density is defined as the number of CaO particles per unit volume of the reactor tube.

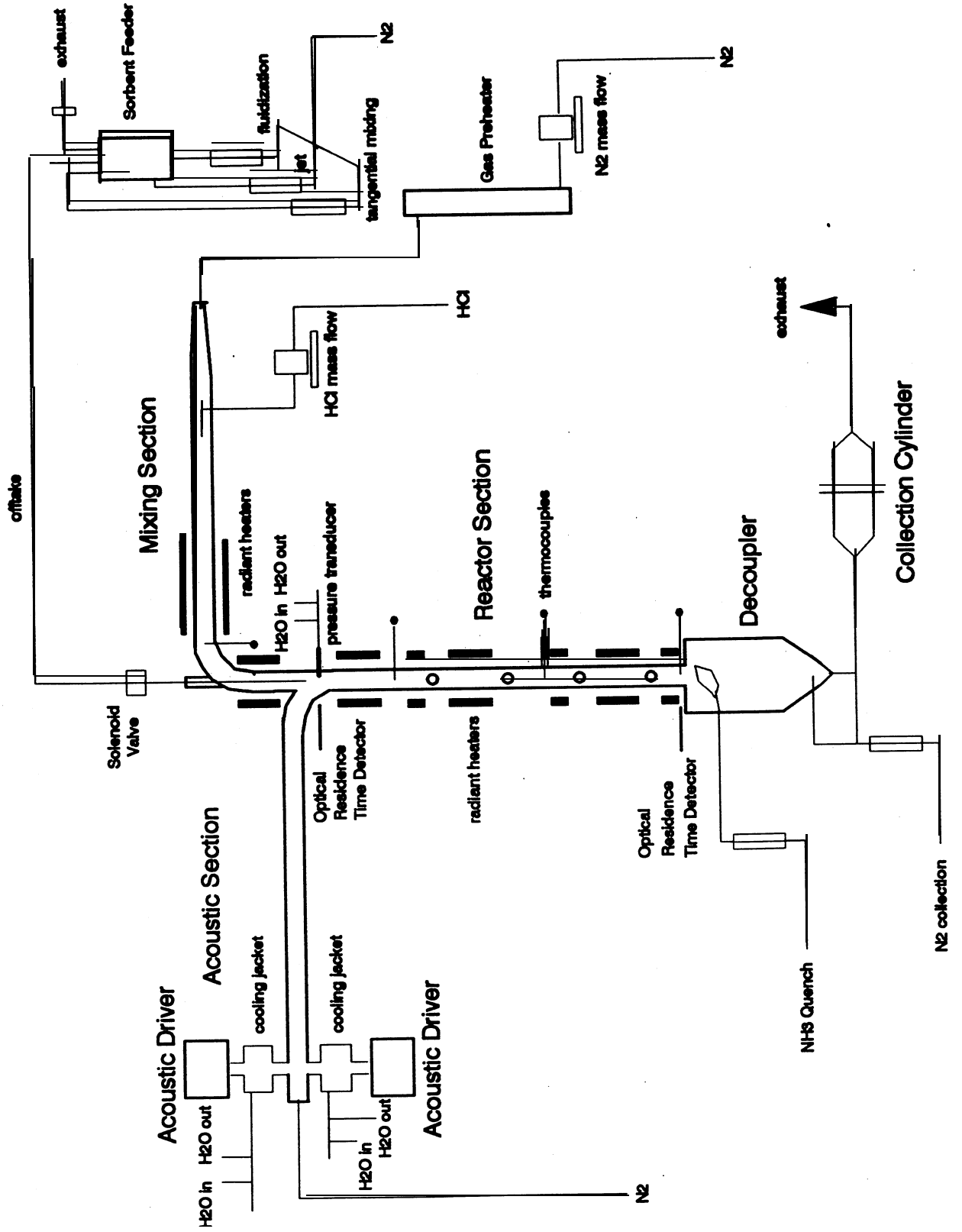

Figure 1. Experimental system schematic (EFK).

3. Materials and Methods

3.1 Hydrogen chloride supply and carrier gas

Dry hydrogen chloride gas and nitrogen from pressure regulated cylinders were monitored through mass flow meters. Nitrogen of 99.998% purity was used as the carrier gas in all experiments. A VLSI electronics grade hydrogen chloride reagent, 99.99% pure, ensures minimization of contaminants. Anhydrous ammonia of 99.99% purity was used to quench unreacted HCl in the reactor decoupler.

3.2 CaO reactant

CaO is the sorbent compound used to react with the HCl gas in the reactor. The CaO reagent contained only trace amounts of magnesium and other ions. Analysis by Inductively Coupled Plasma (ICP) over several samples yielded the following composition of the CaO reagent as presented in Table 1. CaO density is 3.17 g/cm^3.

Table 1. CaO composition.

Compound	Composition, %
CaO	96.5
$CaCO_3$	3.0
MgO	0.5

Calcium oxide pellets of up to 4 mm in diameter were crushed in a ball mill and sifted in a shaker to retain the desired fractions on 125μm, 75μm and 20μm mesh screens. These three size fractions will be referred to throughout the paper as the Large, Medium and Small fractions, respectively. Specific surface area was measured by the BET technique. Mass mean particle size and distribution were determined for each CaO size fraction in Table 2 by a sedimentation method. The distribution range indicates the particle size range of 80% of the particle mass composing a particular CaO fraction. The remaining 20% of mass is below the lowest size in the range given in Table 2. The size distribution is given as an illustration of the composition of the CaO fractions.

Table 2. CaO specific surface area and mean particle size

Mesh Screen Size/ Fraction Name	Specific Surface Area, m^2/g	Distribution Range	Mass Mean Particle Size, μm
20μm / Small	14.7	40μm - 2μm	3.95
75μm / Medium	11.8	110μm - 40μm	55.8
125μm / Large	11.4	150μm - 80μm	90.8

3.3 Ion analysis

Calcium, chloride and ammonium ions were quantitatively determined for the reaction product. The amount of chloride in the product describes the extent of reaction conversion. Ion analysis was performed twice on each reaction product to account for conversion differences resulting from varying size distribution and extent of reaction within a given sample.

Calcium ion was determined by atomic absorption spectroscopy (AA). Chloride and ammonium ions were both determined with an ion selective electrode (ISE). No interfering ions were present in the calcium chloride and ammonium system, thus ISE's were an efficient, accurate method for quantifying chloride and ammonium ion content of a dilute solution. Calcium could be measured with an ISE, but ammonium is an interference to the calcium electrode, thus AA was utilized. Both AA and ISE results for the Cl and Ca ions were expressed in parts per million (ppm). These concentration results were used to calculate the percentage of Cl ion compared to the Ca ions present in the reaction product. The percentage of Cl ion is reported in the reaction conversion figures of this paper.

4. Experimental procedure

CaO fractions, once sifted, were baked in a muffle furnace at 900°C for 1 hour to evaporate bound water to achieve constant weight. Approximately 9g of sample was placed in ceramic crucibles, with no top. Once the sample was dried, it was placed into the particle feeder where the sample was not accessible by water vapor.

Table 3 shows the experimental parameters investigated in this study. The CaO particle size fractions were chosen to cover a wide range of CaO particle sizes. The Small fraction is representative of the size distribution utilized for dry scrubbing applications. The Large and Medium fractions were chosen to discover how they might be affected by an acoustic field. The HCl concentration was chosen to be in a range other investigations have used[7,9,10]. The temperatures chosen represent the range that is optimum for dry scrubbing. The optimum temperature window upper limit for this reaction is 550°C -600°C[8,9,10].

Table 3. Design of two-phase reaction experiments.

CaO Fractions	SPL, dB	HCl Concentration, ppm	Temperature, °C
Small	0	614	125
Medium	160		200
Large			350

At least three replicate experiments were conducted for each case in the experimental matrix. Each EFR experiment was continuously run for 15 minutes and the reaction product collected from the decoupler and collection cylinder. The particle residence time is approximately 0.90 s for each experiment. The flow rate of carrier gas through the reactor was 75 lpm and the concentration of HCl in the carrier gas 614 ppm. Sound pressure level (SPL) was maintained at about 163 dB unless otherwise noted. Variability in flow rates, HCl concentration and SPL was less than 2%. Temperature gradient was less than 3% in the reactor section.

Ion analysis was performed on the reaction product and the precipitate on the collection cylinder screen. No ammonium chloride (NH_4Cl) was found in the reaction product, only calcium and chloride ions. This was due to the physical nature of the CaO particles. The density is sufficiently high that the particles settle at the bottom of the decoupler. The particulates captured in the collection cylinder screen contain chloride and ammonium ions but only a trace of calcium ions. The NH_4Cl precipitate formed upon quenching the unreacted HCl remains entrained in the flow and was captured on the collection cylinder screen. Only the Cl found in the $CaCl_2$ is reported here.

5. Results and discussion

5.1 Product conversion results

A series of experiments was first run to compare the EFR results to other investigations and to establish reproducibility of the data. This was accomplished by running experiments of various CaO size fractions and reactor temperatures. Figure 2 illustrates the behavior of reaction conversion with CaO size fraction, reactor temperature and no sound pressure. Reaction conversion expressed as percent Cl ion in the reaction product is shown over a range of reactor temperature. Chloride ion in the reaction product is calculated as the percentage of chloride present in the product compared to the quantity of calcium in the product.

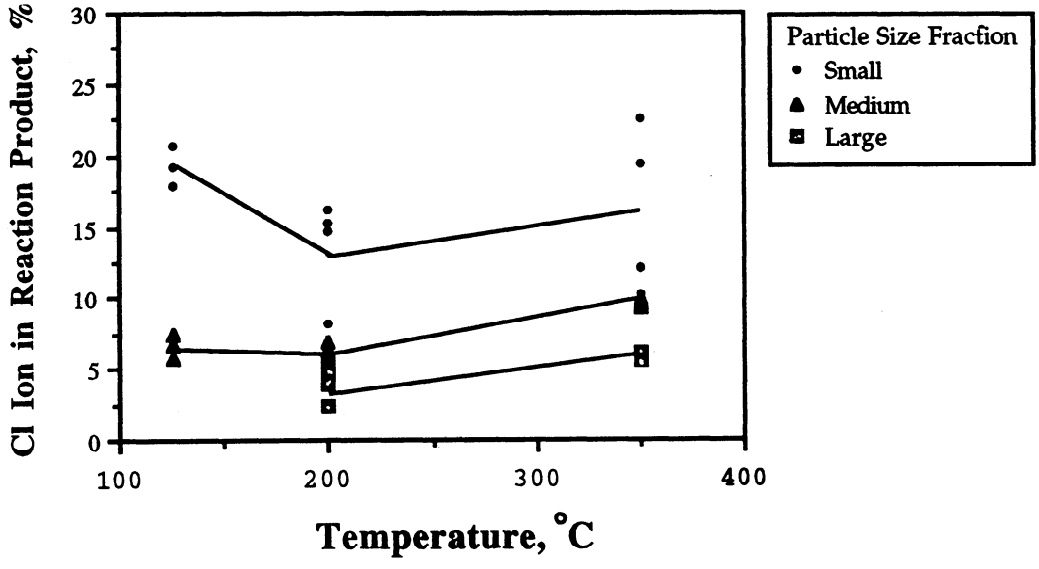

Figure 2 Reaction conversion with respect to sorbent particle size, no acoustics.

Conversion is observed to increase with decreasing CaO particle size and increasing reactor temperature. The Large CaO fraction exhibits little change in conversion with reactor temperature. The Small and Medium CaO fractions do show an increase in reaction conversion with increasing temperature, with a maximum conversion for the Small fraction of 16% at 350°C. The higher conversion for smaller CaO particles is likely due to the greater degree of interior reaction in the smaller particles compared to the larger particle fractions. The importance of the internal reaction plays a greater role as particle size decreases[8]. These results are supported by other investigators who have reported reaction conversion of CaO and HCl to increase with increasing temperature and decreasing CaO particle size[8,9,10].

With a baseline established over a temperature and particle size range, a series of experiments were conducted at 163 dB to determine the effect of sound pressure on reaction conversion. Figures 3-5 illustrate the conversion results expressed as percent Cl ion in the reaction product for the Large, Medium and Small CaO fractions over the temperature range 125°C to 350°C. The 163 dB results are compared to the baseline results of Figure 2.

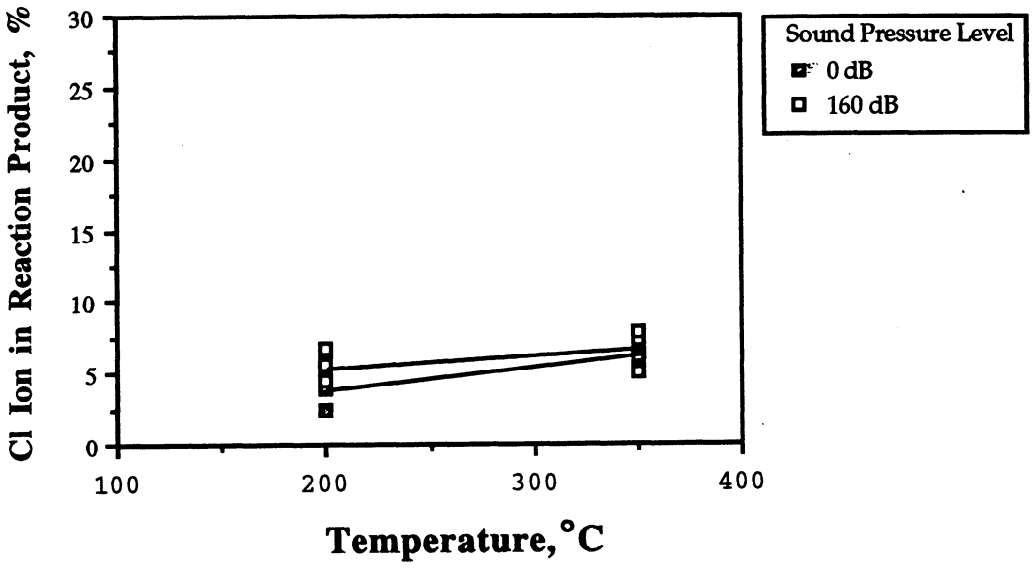

Figure 3 Reaction conversion for Large CaO fraction with and without acoustics.

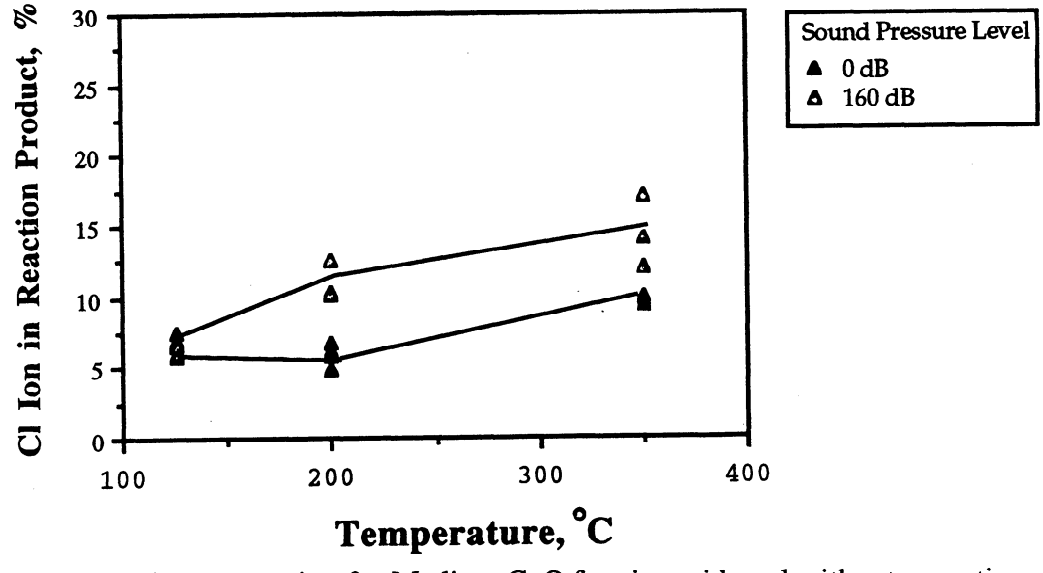

Figure 4 Reaction conversion for Medium CaO fraction with and without acoustics.

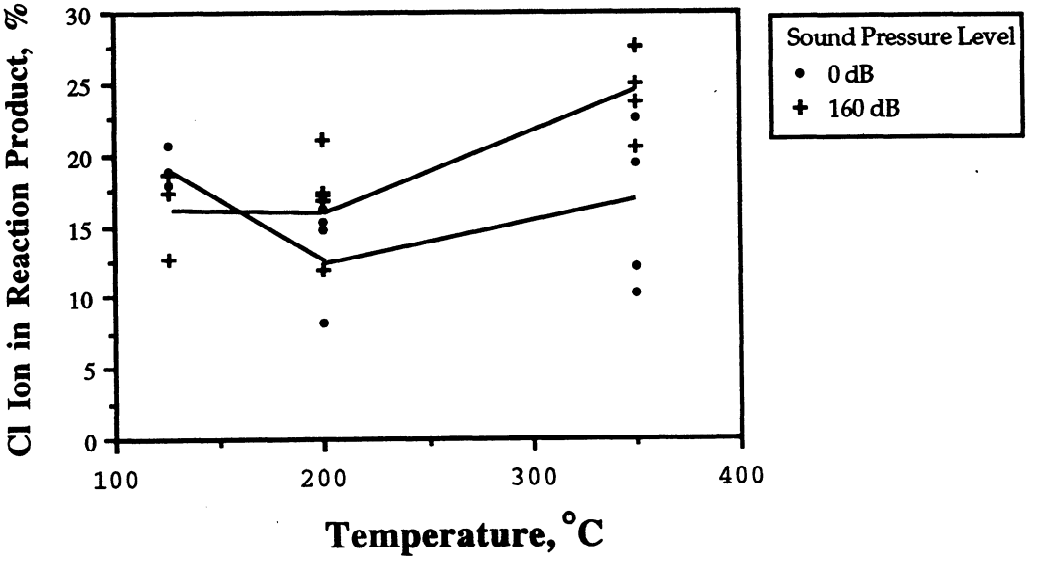

Figure 5 Reaction conversion for Small CaO fraction with and without acoustics.

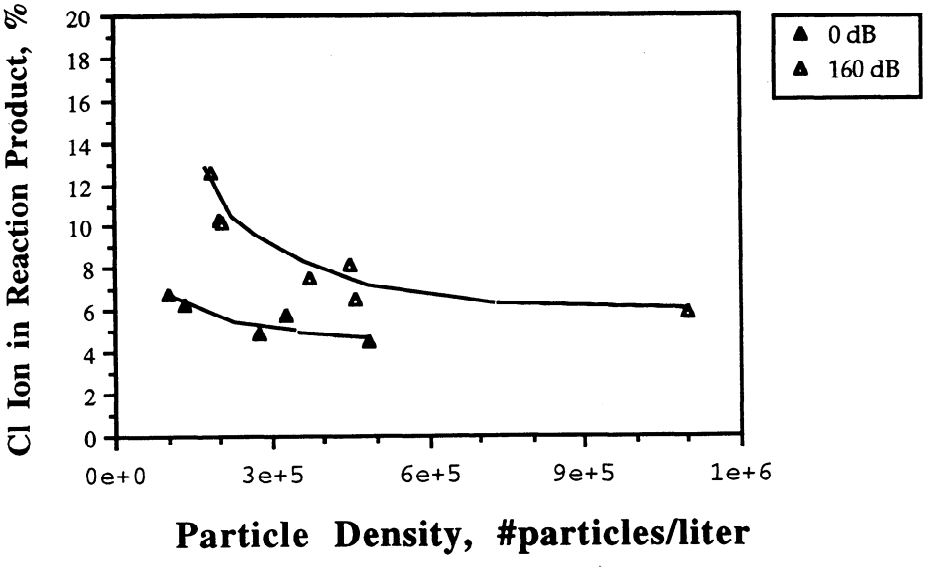

Figure 6 Reaction conversion versus reactor particle density.

Figure 3 shows that reaction conversion in an acoustic field for the Large CaO fraction did not change from the baseline values established in Figure 2. The acoustic field had little effect on the reaction. However, for the Medium CaO fraction in Figure 4, while no change in reaction conversion is evident at 125°C, an appreciable increase has occurred at 200°C and 350°C.

Figure 5 shows the conversion results for the Small CaO fraction under similar reactor conditions and SPL as described for the Large and Medium CaO fractions. A slight improvement in reaction conversion is realized only at 200°C and 350°C. The reaction conversion levels at each temperature with acoustics is similar, indicating that conversion plateaus for the small CaO particles. It is likely that conversion for the Small CaO fraction is maximized due to reaction product porosity affects. The molar volume of $CaCl_2$ is 51.6 cm^3/g while that of CaO is 16.9 cm^3/g[9]. As reaction proceeds, the porosity is reduced. Since the present experiments are at low temperatures to prevent sintering of the CaO particles, porosity reduction results from reaction progression as more $CaCl_2$ is formed.

Data scatter is quite evident for the Small CaO fraction and may be linked to the variability of CaO size distribution and particle density in the reactor between experiments. Particle density refers to the number of CaO particles per liter (number particles/liter) of reactor volume during an EFR experiment. The variability is evident from the COV presented in Table 4. Care must be taken to consistently achieve similar particle density for each experimental case in order to ensure comparison of similar conditions for both the acoustics and nonacoustics cases.

The particle density concept is illustrated in Figure 6 where the Medium CaO fraction, 200 °C case with and without acoustics over a range of particle densities were intentionally run to examine the particle density effect. The figure shows that as particle density increases, conversion drops for the cases both with and without acoustics. Above $3.3x10^5$ particles/liter conversion drops rapidly and significantly for the experiments with acoustics where the conversion varies from a high of 12% and drops to almost 6.5% at the highest particle density. Without acoustics, the percent of chloride ion in the reaction product ranges from 4.5% to 6.5%. If the particle densities are maintained in the range $0.85x10^5$ - $3.3x10^5$ particles/liter, conversion is fairly consistent as illustrated in the no 0dB case. Comparison can be made of the no acoustics case to the case with acoustics in this particle density range, eliminating conversion differences between experiments due to the number of CaO particles present.

Particle density for the Large CaO fraction was maintained between $0.23x10^5$-$1.42x10^5$ particles/liter. No specific particle density range was found to be necessary for the Small CaO fraction. In other words, conversion did not vary with particle density for the Small CaO fraction. Particle density for the Small fraction ranged from $7.65x10^5$ to $113x10^5$ particles/liter.

Figure 7 illustrates the difference in reaction conversion due to 163 dB SPL while altering the CaO particle size fraction and reactor temperature. It is evident that as average CaO particle size decreases, reaction conversion increases. This is the trend that was evident for the cases with no sound pressure in Figure 2, only a higher conversion is achieved with the use of acoustics as was indicated in the above discussion.

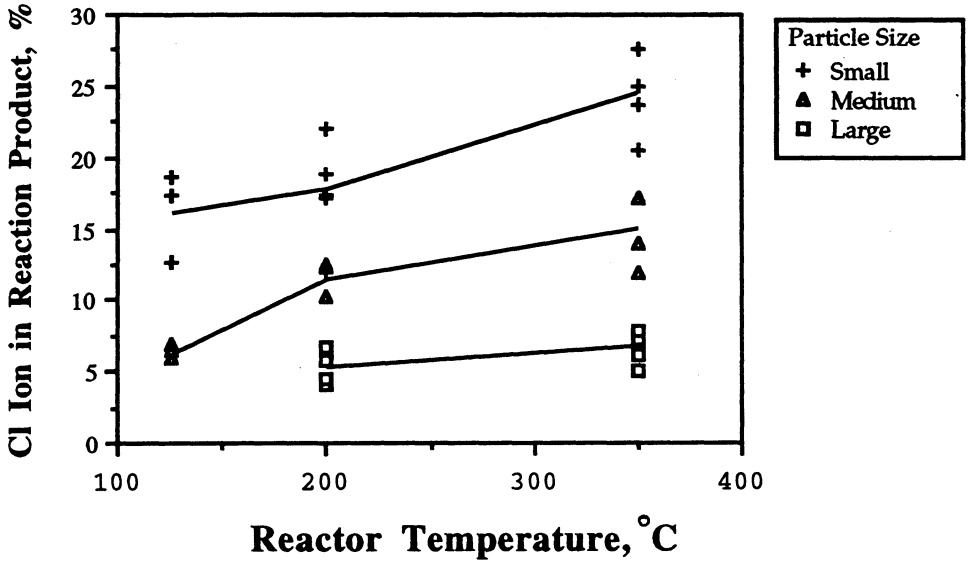

Figure 7 Reaction conversion by CaO particle size fraction with acoustics.

The data from Figures 3 - 5 are listed in Table 4. The average conversion, standard deviation and coefficient of variation is listed at each condition of temperature and average particle size. The change in reaction conversion due to SPL is tested for significance by using a T-test to compare the difference in average value at each experimental condition.

Table 4 Experimental data: statistical presentation for all CaO fractions.

Large CaO	0 dB			160 dB		
Reactor Temperature °C	Average conversion %	Std Dev.	COV %	Average conversion %	Std Dev.	COV %
200	4.08	1.09	25.7	5.44	1.19	21.87
350	5.90	0.26	4.32	6.53	1.05	16.09

Table 4 continued.

Medium CaO	0 dB			160 dB		
Reactor Temperature °C	Average conversion %	Std Dev.	COV %	Average conversion %	Std Dev.	COV %
125	6.68	0.69	10.27	6.36	0.44	6.97
200	5.95	0.82	13.73	11.02	1.32	12.01
350	9.62	0.30	3.07	14.37	2.58	17.95

Small CaO	0 dB			160 dB		
Reactor Temperature °C	Average conversion %	Std Dev.	COV %	Average conversion %	Std Dev.	COV %
125	22.48	5.61	24.94	16.17	3.17	19.61
200	13.62	3.65	26.77	16.86	3.23	19.16
350	16.11	5.88	36.47	24.17	3.01	12.45

The difference between the mean reaction conversion for the Large CaO fraction with and without acoustics is not significant. However, the Medium CaO fraction at 200°C and 350°C exhibits a significant difference between the means according to the t-test at 95% confidence. No significant difference in means is found for the Small CaO fraction at any reactor temperature. Improvement in reaction conversion is demonstrated under certain conditions of temperature and CaO fraction. The hypothesis for the improved conversion is examined next.

5.2 Change of SPL and reaction conversion

SPL was investigated to determine if this was a factor in creating the conversion enhancement evident from the acoustic field. Previous investigations reported values of 140 to 160 dB necessary to achieve improvements in various reaction systems under investigation[5,6]. For this work, two additional levels of SPL were chosen, 140dB and 150dB. Table 7 shows the reaction conversion for the Medium CaO fraction at 200°C.

Table 7: Reaction conversion at various SPL.

SPL, dB	Cl Conversion, %
0	5.95
140	6.06
150	6.04
160	10.62

The data suggests that a threshold SPL exists at 160 dB. No conversion changes are evident at 140 dB or 150 dB as compared to the base case conversion. However, conversion increases for SPL above 160 dB. A threshold SPL of 160 dB is evident for the CaO/HCl reaction. Some phenomenon related to SPL seems responsible for the improved reaction conversion of the Medium CaO fraction.

5.3 Turbulence in an acoustic field

Measurement of SPL in the reactor section of the EFR with a pressure transducer revealed sound pressure nodes of 160 - 163 dB approximately every 12 inches. The pressure nodes are maximum sound pressure areas established as a result of the 600-750 Hz frequency range used in these experiments. Visually, particles injected into the reactor system can be seen mixing in these regions, then flowing to the next mixing region and so on until the particles reach the bottom of the reactor. Zones of acceleration and zones of mixing are observed throughout the length of the EFR tube due to the sound pressure nodes. Figure 8 illustrates the mixing hypothesis.

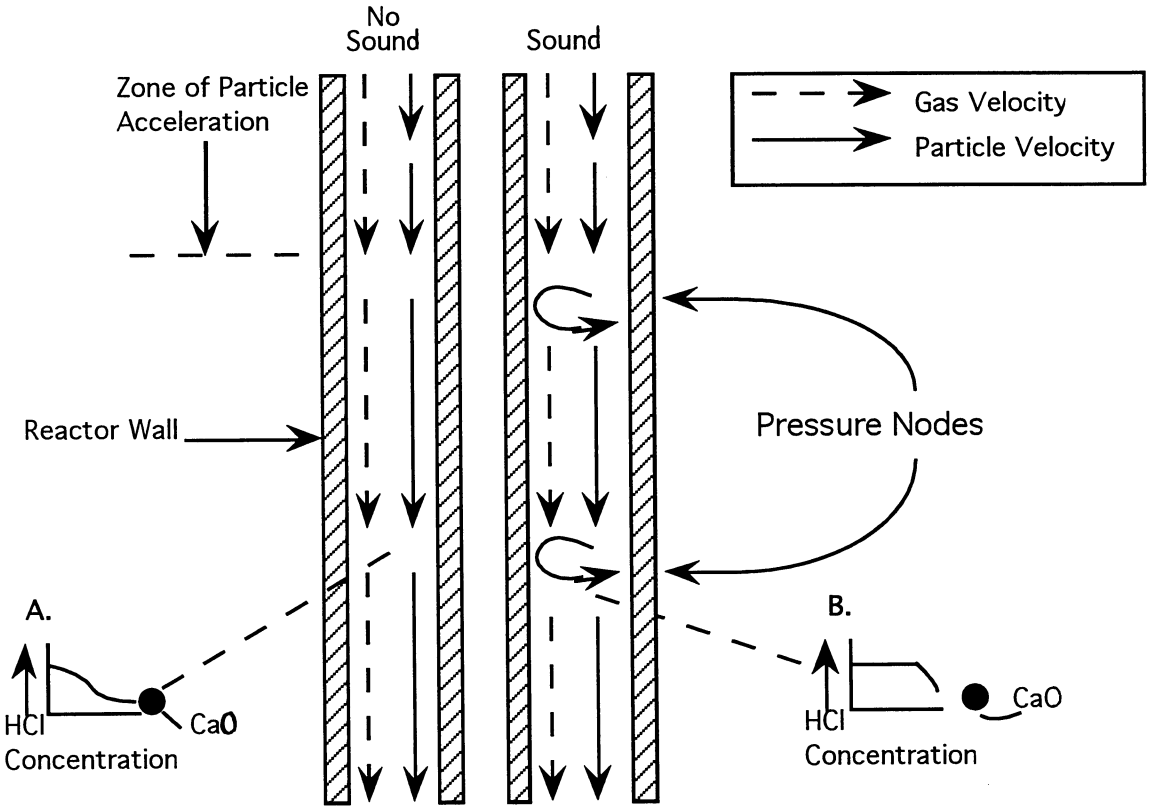

Figure 8 Mixing hypothesis

Without acoustics the CaO particles accelerate to the carrier gas velocity. With acoustics a region of maximum sound pressure (node) will possess a minimum particle and gas velocity, but a region of minimum sound pressure will possess a maximum gas and particle velocity. The flow of nitrogen carrier gas through the reactor is constant for all experiments, so average residence time should not change appreciably in the acoustic

field, though regions of gas and particle deceleration and acceleration occur. It is in the alteration of gas and solids slowing and speeding that mixing seems to occur. The flow field established due to the variable acoustic pressure creates turbulence and can be characterized by the quantity turbulence intensity.

Turbulence intensity is defined as[11]

$$I \equiv \frac{(1/3\overline{u_i u_i})^{1/2}}{U_o}$$

where u is the component velocity and U_o the mean flow velocity. Turbulence intensity can be defined for each velocity component as the root mean square referenced to a mean flow velocity. Turbulence intensity levels measured by laser doppler velocimetry for the downward flow component shows that turbulence intensity increases above 140 dB SPL according to measurements provided in Table 8. It is hypothesized that the increased turbulence improves the mixing of the gas phase to improve the reactant gas concentration gradient around the CaO particle.

Table 8 Turbulence intensity

SPL, dB	Turbulence Intensity, %
0	3-8
133	3-5
140	18-33
160	19-32

In steady flow, HCl concentration around a single CaO particle may steadily decrease from the bulk phase concentration to zero near the particle surface, as depicted in Figure 8A. However, in an acoustic field, the improved mixing may improve the concentration of reactant gas around the CaO particle as shown in Figure 8B. A greater HCl concentration will present more HCl to the CaO particles for reaction. However, if better mixing as illustrated through turbulence intensity was the only reason for mass transfer improvement to the CaO/HCl reaction, we would expect to see greater reaction conversion at 140 dB and not only 160 dB. Another, yet to be identified, phenomenon must be responsible for improving mass transfer to the CaO particles to improve reaction conversion. Perhaps SPL and the mixing phenomena combine to improve mass transfer to the CaO particles.

6. Conclusions

Conversion is enhanced by conducting the CaO/HCl reaction in an acoustic field over 160 dB. As stated previously, the Large CaO fraction does not experience a significant improvement in reaction conversion with acoustics. The Medium and Small fractions do experience some improvement in reaction conversion with acoustics above 200

°C reactor temperature. The conversion improvement is statistically significant for the Medium fraction. Only a marginal conversion increase is realized for the Small fraction.

Conversion improvement is likely due to an improvement in mass transfer of HCl to the CaO particle. Turbulence intensity levels found in the resonant acoustic field increase dramatically from 3-8% to over 30% above 140 dB. Mixing in the gas phase may improve the concentration gradient of the gas to the solid particle. Further theoretical development is required to fully illustrate the mass transfer phenomenon.

Application of acoustics to any gas-solid reaction to enhance reactant mixing may be possible for the correct combination of parameters such as SPL, frequency, particle size, temperature and reaction time requirements.

7. Future Work

Future work will involve measuring porosity for the Small CaO fraction for both reacted and unreacted samples to establish whether maximum conversion is limited by porosity reduction. A theoretical model will be proposed to account for mass transfer affects in a gas/solid reaction system to determine how mass transfer is affected by the acoustic field for the CaO/HCl reaction.

8. Acknowledgments

Financial support of this work by the Institute of Paper Science and Technology and its Member Companies is gratefully acknowledged. Portions of this work will be used by J.B. for the Ph.D. degree at the Institute of Paper Science and Technology.

9. Literature Cited

1. Jozewicz W.; Chang, J.C.S. Bench-scale evaluation of calcium sorbents for acid gas emission control. Environmental Progress 9(2):137-142 (August 1990)

2. Del Bueno, D.; Seay, R. Tighter sulfur dioxide regulations spur better control technologies. Pulp & Paper 63(9):190-194 (September 1989)

3. Michele, H. Purification of flue gases by dry sorbents-possibilities and limits. International Chemical Engineering 27(2):183-196 (April 1987)

4. Muzio, L.J.; Offen, G.R. Assessment of dry sorbent emission control technologies. Part I. Fundamental processes. JAPCA 37(5):642-654 (May 1987)

5. Zinn, B.T.; Dubrov, E.; Rabhan, A.B.; Daniel, B.R. Application of resonant driving to increase the productivity and thermal efficiency of industrial processes. Proceedings of the International Symposium on Pulsating Combustion, August 5-8 1991

6. Stewart, C.R.; Lemieux, P.M.; Zinn, B.T. Application of pulse combustion to solid and hazardous waste incineration. Proceedings of the International Symposium on Pulsating Combustion, August 5-8 1991

7. Daoudi, M; Walters, J.K. A thermogravimetric study of the reaction of hydrogen chloride gas with calcined limestone: determination of kinetic parameters. The Chemical Engineering Journal 47 :1-9 (1991)

8. Daoudi, M; Walters, J.K. The reaction of HCl gas with calcined commercial limestone particles: the effect of particle size. The Chemical Engineering Journal 47 :11-16 (1991)

9. Mura, G.; Lallai, A. On the kinetics of dry reaction between CaO and gas HCl. Chemical Engineering Science 47(9):2407-2411 (1992)

10. Weinell, C.E.; Jensen, P.I.; Dam-Johansen, K.; Livberg, H. Hydrogen chloride reaction with lime and limestone: kinetics and sorption capacity. Industrial Engineering Chemistry Research 31:164 - 171 (1992)

11. Panton, R.L. Incompressible Flow. John Wiley & Sons, Inc., 1984.